

Article

Impacts of Modified Fly Ash on Soil Available Lead and Copper and Their Accumulation by Ryegrass

Hongbiao Cui ^{1,2,3}, Xue Sheng ^{1,2,3}, Shaojun Hu ^{1,2,3}, Shuai Li ^{1,2,3}, Shiwen Zhang ^{1,2,3} and Jun Zhou ^{4,*}

¹ School of Earth and Environment, Anhui University of Science and Technology, Huainan 232001, China; hbcui@aust.edu.cn (H.C.); 2022200032@aust.edu.cn (X.S.); 17775209610@163.com (S.H.); 19155440675@163.com (S.L.); shwzhang@aust.edu.cn (S.Z.)

² Engineering Laboratory of Anhui Province for Comprehensive Utilization of Water and Soil Resources and Construction of Ecological Protection in Mining Area with High Groundwater Level, Anhui University of Science and Technology, Huainan 232001, China

³ Academician Workstation in Anhui Province, Anhui University of Science and Technology, Huainan 232001, China

⁴ Key Laboratory of Soil Environment and Pollution Remediation, Institute of Soil Science, Chinese Academy of Sciences, Nanjing 210008, China

* Correspondence: zhoujun@issas.ac.cn

Abstract: Fly ash (FA) is promising for environmental remediation, but how to modify the FA with high remediation efficiency through an environmentally friendly and low-cost modification method is scarce. A modified FA (MFA) was prepared through a one-step hydrothermal modification with $\text{Ca}(\text{OH})_2$ and KH_2PO_4 . Results indicated that irregular agglomerates occurred on the surface of the MFA and that the specific surface area increased by 1.94 times compared to that of FA. Compared to FA, glassy compositions in MFA were destroyed and amorphous Si/Al and alkaline aluminosilicate gels were formed. The soil application of 0.2–0.6% MFA significantly increased soil pH by 0.23–0.86 units compared to FA and decreased available lead (Pb) and copper (Cu) by 25–97.1% and 13.5–75%, respectively. MFA significantly decreased exchangeable Pb and Cu by 12.5–32% and 11.4–35.2%, respectively, compared to FA. This may be due to the high pH and specific surface area of MFA, which promoted to the formation of amorphous Si/Al, metal–phosphate precipitation, and complexation with functional groups. In addition, MFA slightly increased the biomass of shoots and roots and decreased the uptake of Pb and Cu by ryegrass. This study provides a new modification method for the utilization of FA in the heavy metal-contaminated soils.

Keywords: fly ash; Pb and Cu; passivation; accumulation; ryegrass



Citation: Cui, H.; Sheng, X.; Hu, S.; Li, S.; Zhang, S.; Zhou, J. Impacts of Modified Fly Ash on Soil Available Lead and Copper and Their Accumulation by Ryegrass. *Agronomy* **2023**, *13*, 2194. <https://doi.org/10.3390/agronomy13092194>

Academic Editor: Pablo Martín-Ramos

Received: 22 July 2023

Revised: 16 August 2023

Accepted: 19 August 2023

Published: 22 August 2023



Copyright: © 2023 by the authors. Licensee MDPI, Basel, Switzerland. This article is an open access article distributed under the terms and conditions of the Creative Commons Attribution (CC BY) license (<https://creativecommons.org/licenses/by/4.0/>).

1. Introduction

Coal-fired power plants are still the main source of electricity in many countries worldwide and the generation is estimated to account for 46% of the global electricity supply by 2030 [1]. China is the largest consumer of coal in the world, and the coal consumption accounts for 56% of the country's total energy consumption in 2021 [2,3]. Meanwhile, considerable amounts of fly ash (FA) are generated from coal-burning power plants. In 2012, nearly 750 million tons of FA were produced annually worldwide [4], and the increasing demand for energy has caused an alarming rise in FA production. The output of FA was nearly 620 million tons in China in 2015 [5], which has become the largest single source of solid pollution [1,6]. Although the worldwide production of FA has slightly decreased in recent years, the utilization rate of FA has remained at a relatively low level [7]. In fact, there is a considerable amount of FA stored in stockpiles, landfills, and ponds, causing seriously environmental issues [8]. Inappropriate disposal and long-term natural exposure of FA causes severe air, soil, and water pollution, and is hazardous to plant growth and human health [9]. Therefore, it is crucial to explore new utilization methods for FA.

FA is mainly utilized in road construction, brick manufacture, the concrete industry, and agricultural fields [10,11]. It can be used as an alternative for the adsorption of heavy metals owing to its low cost, high porosity, high specific surface area, and iron/aluminum oxides [11]. However, the adsorption capacity of heavy metals by FA is relatively low. For example, the removal of copper (Cu) ions by FA was only 1.4 mg g^{-1} , which was significantly less than that of NaOH-treated FA (58.48 mg g^{-1}) [12,13]. Cui et al. [14] reported that 0.2–2% FA increased soil pH, but only 2% of FA significantly decreased the exchangeable Cu and cadmium (Cd), by 35.7% and 35.9%, respectively. Therefore, it is indispensable to improve its adsorption capacities via modification methods. Xu et al. [15] used a low-temperature roasting method to modify FA, and soil application of the new FA at a 2% rate decreased the available lead (Pb) by 30–48.3%. Nevertheless, the majority of previous modification methods were complicated, time consuming, had high energy consumption, and even led to secondary pollution, which limited the reuse of FA on a large scale [16–18]. Therefore, it is important to develop environmentally friendly and low-cost modification methods for FA.

Simple alkali modification of FA increased the specific surface area of FA from $1.45 \text{ m}^2 \text{ g}^{-1}$ to $31.6 \text{ m}^2 \text{ g}^{-1}$, and the adsorption capacity of Pb^{2+} and Cd^{2+} increased by 41.9% and 92.5%, respectively [19]. Numerous studies have demonstrated that phosphorus-rich materials can be used as amendments in heavy metal-contaminated soils since they can form metal–phosphate precipitation with low solubility and high buffering stability [20–22]. For example, Cao et al. [23] suggested that phosphate amendments could promote the immobilization of Pb in soils and decreased the toxicity characteristic leaching procedure of extractable Pb by 89.2%. Our previous studies also found that soil CaCl_2 -extractable Pb, Cu, and Cd were decreased by 99.4%, 95%, and 79%, respectively, in potassium dihydrogen phosphate-treated soils [24].

Therefore, we prepared a new modified FA (MFA) by one-step co-precipitation of $\text{Ca}(\text{OH})_2$ and KH_2PO_4 in this study. This study aims (1) to investigate the passivation effects of Pb and Cu by MFA in contaminated soil and (2) to evaluate the effects of MFA on the biomass and metal accumulation of ryegrass. This study will provide a new potential utilization direction for FA in environmental remediation.

2. Materials and Methods

2.1. Experimental Materials

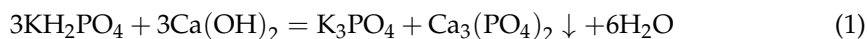
Original FA samples were collected from the Luohe Power Plant in Huainan, China. The pH of FA was 12.4 and the distribution of particle sizes of <5, 5–10, 10–20, 20–30, 30–50, and >50 μm were 7.85%, 20.6%, 42.2%, 10.6%, 9.62%, and 9.13%, respectively. Total Pb and Cu in FA were 40.1 mg kg^{-1} and 67.3 mg kg^{-1} , respectively.

The soil samples were collected from an abandoned agricultural land near a Cu smelter in Guixi, China. Soil samples were air-dried and then ground through a 10-mesh sieve for the pot trial. Soil pH, organic carbon, cation exchange capacity (CEC), total Pb, and total Cu were 3.67, 13.1 g kg^{-1} , $89.5 \text{ mmol kg}^{-1}$, 1331 mg kg^{-1} , and 635 mg kg^{-1} , respectively. Ryegrass is a suitable species for the revegetation of heavy metal-contaminated soils [25]; thus, we planted ryegrass in the contaminated soil. Annual ryegrass (*Lolium Perenne* L.) seeds were purchased from a seed distributor. All chemicals used in this study were analytical grade and purchased from Sinopharm Chemical Reagent Co., Ltd. (Nanjing, China).

2.2. Preparation of MFA

The original FA was modified with $\text{Ca}(\text{OH})_2$ and KH_2PO_4 under hydrothermal conditions. $\text{Ca}_3(\text{PO}_4)_2$ was anticipated to form through the reaction between $\text{Ca}(\text{OH})_2$ and KH_2PO_4 (Equation (1)), and the theoretical mass ratio was 1.41:2.59 based on the purity of $\text{Ca}(\text{OH})_2$ and KH_2PO_4 . Our preliminary experiment showed that the MFA prepared with a mass ratio of $\text{FA}:\text{Ca}(\text{OH})_2:\text{KH}_2\text{PO}_4 = 20:1.41:2.59$ had higher adsorption capacities for Pb and Cu than that of 36:1.41:2.59, but lower than that of 8:1.41:2.59. Considering the cost, we synthesized the MFA by weighting 20 g FA, 1.41 g $\text{Ca}(\text{OH})_2$, and 2.59 g KH_2PO_4 in

a beaker and then mixed it well with 240 mL deionized water for 1 h. Subsequently, the beaker was heated in a water bath at 100 °C for 24 h, and then the suspensions were cooled and centrifuged and the solid residue was washed with distilled water until a stable pH was reached (10 ± 0.10). Finally, the resulting MFA was oven-dried at 60 °C, ground, and passed through a 100-mesh sieve.



2.3. Incubation Experiment

The incubation experiment was conducted in 1 L polyvinyl chloride (PVC) tanks (10 cm (D) × 15 cm (H)) containing 3000 g of contaminated soil. Considering the economic cost and operability of practical field application, FA and MFA were added to the soil at low dosages of 0.2%, 0.4%, and 0.6% (*w/w*) [14]. There were seven treatments, including control (CK), 0.2% FA (FA-2), 0.4% FA (FA-4), 0.6% FA (FA-6), 0.2% MFA (MFA-2), 0.4% MFA (MFA-4), and 0.6% MFA (MFA-6). Meanwhile, 3.0 g basal fertilizer (N:P₂O₅:K₂O = 15:15:15) were manually mixed with the soils. The soil moisture in all treatments were maintained at 70% of the maximum water-holding capacity. Three replicates were performed for each treatment. Then, 20 germinated ryegrass seeds (*Lolium Perenne* L.) were sowed into the tanks and cultured in a light incubator at 25 ± 2 °C with a relative humidity of 70%, an illuminance of 8000 lux, and a photoperiod of 12 h light/dark. The ryegrass was harvested and then washed with tap water and deionized water after incubation for 30 days.

Soil pH and CaCl₂-extractable Pb and Cu were determined on the 7th, 14th, 21th, and 30th days. The speciation of Pb and Cu in soils was determined on the 30th day. In addition, the harvested ryegrass was separated into shoot and root parts, and the biomass and total Pb and Cu concentrations in ryegrass were also determined on the 30th day.

2.4. Chemical Analysis

The scanning electron microscope (SEM), the Brunauer–Emmett–Teller (BET), Fourier transform infrared spectroscopy (FTIR), X-ray photoelectron spectroscopy (XPS), and X-ray diffraction (XRD) analysis were carried out based on Cui et al. [26], and detailed information can be found in Text S1.

The pH of FA, MFA and soil were determined using a pH meter (PHS-25, Leici, Shanghai, China) with a liquid–solid ratio of 2.5:1. Soil organic carbon and cation exchange capacity (CEC) were analyzed according to the methods of Walkley and Black [27] and Pansu and Gautheyrou [28], respectively. Soil available silicon (Si) was determined by the silicon–molybdenum blue colorimetric method [29]. Total Pb and Cu in FA, MFA and soil were measured by a flame or graphite furnace atomic absorption spectrophotometer (A3, Persee General Instrument, Beijing, China) after the samples were digested with an acid mixture (HNO₃-HF-HClO₄: 5-10-5 mL) [30]. Soil available Pb and Cu were extracted by 0.01 mol/L CaCl₂ in a solid–liquid ratio of 1:5 (*w/v*) [31]. The sequential extraction procedure was used to analyze the five types of speciation of soil Pb and Cu, including exchangeable (EXC), binding to carbonate (CA), iron and manganese oxide (Fe-Mn), organic matter (OM), and residual (RES) [32]. For more detailed information on the sequential extraction procedure, refer to Text S2.

The shoots and roots of ryegrass were digested with an acid mixture (9 mL HNO₃:1 mL HClO₄) based on our previous study [33], and the total Pb and Cu concentrations in the digestion solution were determined using a flame or graphite furnace atomic absorption spectrophotometer.

For quality assurance, all tests were conducted in triplicate. Blanks, along with certified soil (GBW07405, Nanjing, China) and plant (GBW10010, Nanjing, China) reference materials, were analyzed, and the recovery rate ranged from 93% to 107%.

2.5. Data Analysis

Statistical analysis was performed using IBM Statistical Product and Service Solutions (SPSS) Statistics 26.0. All results were expressed as mean \pm standard error. The significant differences among the treatments were identified by Duncan's honestly significant difference test ($p < 0.05$) via one-way ANOVA. All figures were created using Origin 2021.

3. Results and Discussion

3.1. Characterizations of FA and MFA

The surface of FA exhibited a loose structure and was primarily composed of smaller spherical powder particles with varying sizes and relatively smooth appearances (Figure 1A). However, the glass-phase structure in MFA was disrupted and resulted in some irregular agglomerates with rough external morphology (Figure 1B). Consistent with the SEM results, the specific surface area of MFA ($18.6 \text{ m}^2 \text{ g}^{-1}$) was increased by 1.94 times compared to that of FA ($9.57 \text{ m}^2 \text{ g}^{-1}$). The increase in specific surface area for MFA may have been due to the destruction of the silica–aluminate structure of FA through the dissolution of the surface glass under $\text{Ca}(\text{OH})_2$ [34].

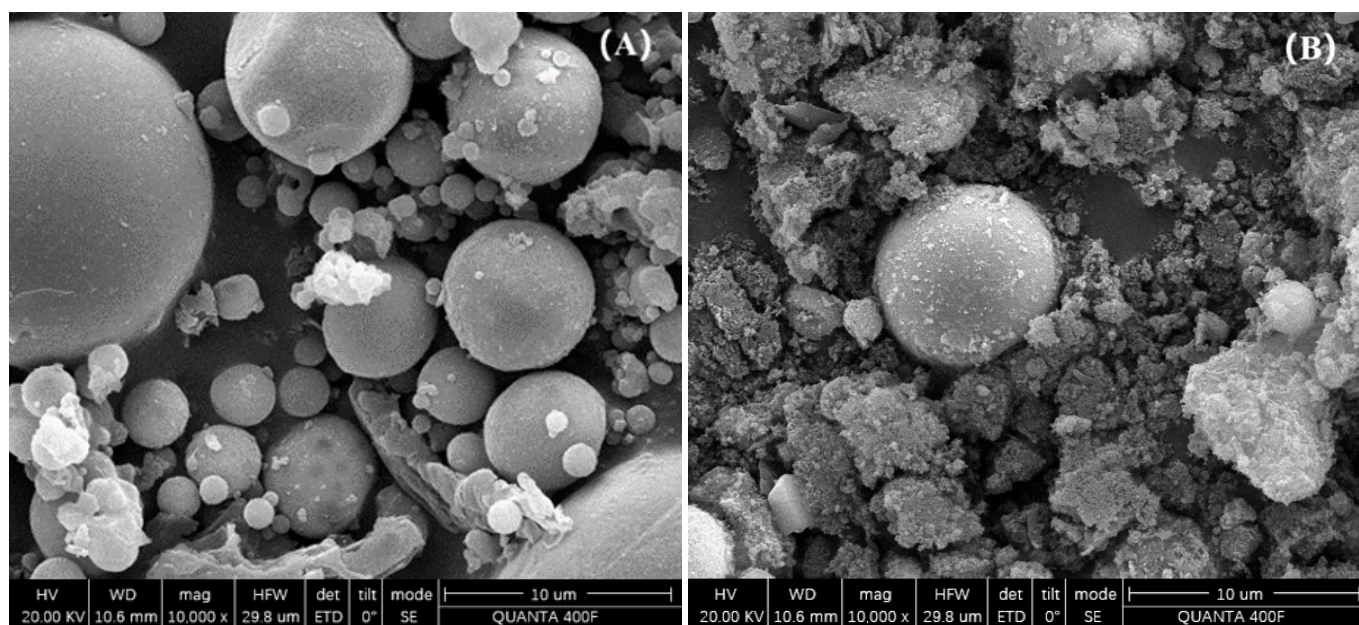


Figure 1. The SEM images of FA (A) and MFA (B). Note: FA: fly ash; MFA: modified fly ash.

FA and MFA mainly consisted of mullite ($3\text{Al}_2\text{O}_3 \cdot 2\text{SiO}_2$), quartz (SiO_2), and hematite (Fe_2O_3) (Figure 2A). A broad characteristic diffraction peak appeared between 25° and 30° , indicating the presence of vitreous humor in FA and MFA [34,35]. The diffraction peaks of mullite and quartz decreased after modification, demonstrating that stable substances such as $\text{SiO}_2/\text{Al}_2\text{O}_3$ were activated. The reason is that the Si-O and Al-O were broken down by the high concentration of OH^- , which released the active negatively charged groups [36]. Furthermore, numerous diffusive peaks with diminished diffraction intensity were observed, and their intensity was decreased compared to that of the original FA, indicating that a portion of the glass structure in FA was disrupted during the modification process [37]. The active Al_2O_3 and SiO_2 in MFA can act as adsorbents, thus increasing the adsorption capabilities of MFA [38]. Unlike in FA, new peaks of calcite (CaCO_3) appeared between 25° and 30° in MFA, which may have been due to the reaction of carbon dioxide (CO_2) with alkaline material present in the FA [39]. However, phosphate minerals ($\text{Ca}_3(\text{PO}_4)_2$) were not determined in MFA. This was mainly due to the concentration of phosphate being below 2–5%, which is less than the detection limit of XRD [40].

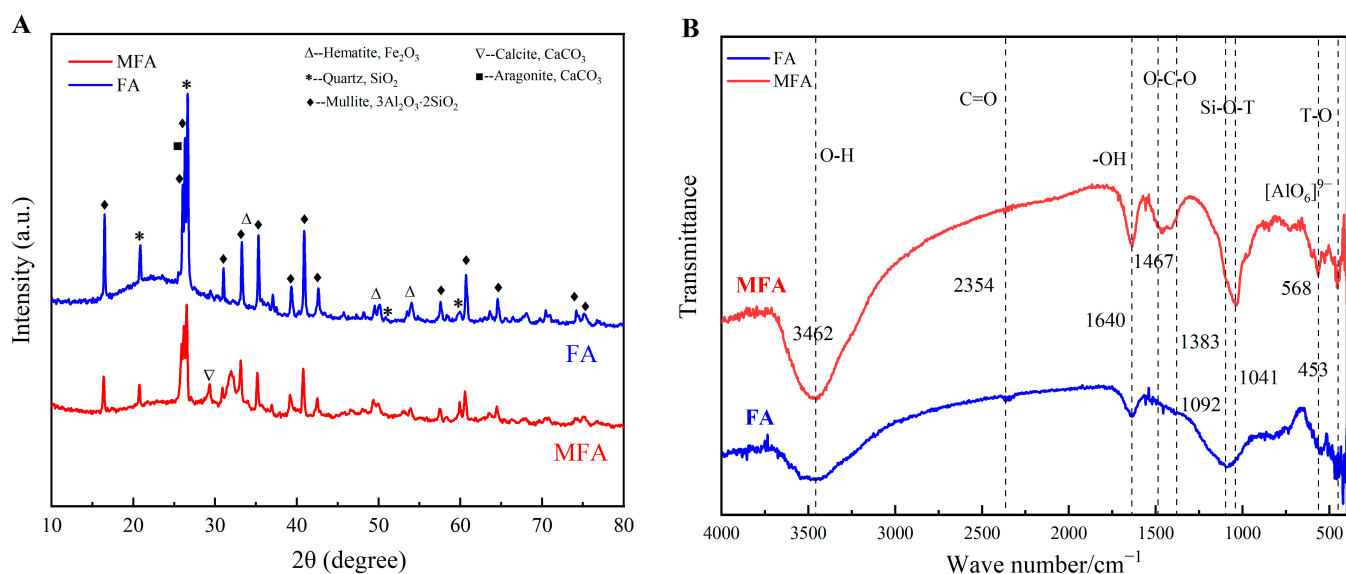


Figure 2. Spectrums of XRD (A) and FTIR (B) for FA and MFA. Note: FA: fly ash; MFA: modified fly ash.

The main functional groups in FA included -OH (3462 cm⁻¹), C=O (2354 cm⁻¹), -OH (1640 cm⁻¹), Si-O-T (T=Si, Al) (1092 cm⁻¹), [AlO₆]⁹⁻ octahedral structure (568 cm⁻¹), and T-O (T=Si, Al) (453 cm⁻¹) (Figure 2B). Unlike in FA, two strong and broad peaks appeared at 1640 cm⁻¹ and 3462 cm⁻¹ in MFA, which were related to -OH stretching vibration [41]. In addition, the peak of the asymmetrical stretching vibration of Si-O-T (T=Si, Al) in MFA became sharper and red-shifted from 1092 cm⁻¹ to 1041 cm⁻¹. This result indicates that the glassy compositions of FA (SiO₂ and silica–alumina compounds) were successfully modified and formed some alkaline aluminosilicate gels [42]. Moreover, the O-C-O stretching vibration peak was increased at 1467 cm⁻¹ for MFA, indicating that the modification procedure increased the species of oxygen-containing functional groups [43].

The XPS spectra indicated that C, O, Al, Si, Ca, and P were mainly present on the surface of MFA (Figure 3). The shifts in the O (1s), Ca (2p), P (2p), and Si (2p) peaks indicate that there were variations in the speciation of oxygen, phosphate, iron oxides, phosphate minerals, and quartz [44]. The Ca (2p) peak was detected after modification, indicating that Ca²⁺ was retained in MFA [31]. After modification, the Si/Al binding energies of the corresponding spectral bands in MFA were 102.48 eV and 74.11 eV, which were reduced by 0.50 eV and 0.47 eV more than in FA, respectively (Figure S1). The stronger Si/Al peaks in MFA than in FA suggest that the dissolution of the Si/Al functional group in the glass phase resulted in the formation of amorphous Si/Al [44,45].

3.2. Soil pH, CaCl₂-Extractable, and Chemical Speciation of Pb and Cu

During the incubation process, the application of FA and MFA significantly increased soil pH by 0.07–0.30 and 0.35–1.11 units compared to the control ($p < 0.05$) (Figure 4A). Compared to FA, soil pH was significantly increased by 0.23–0.86 units with an MFA dosage from 0.2% to 0.6% and continuously increased with time. For example, MFA-4 significantly increased soil pH by 0.39–0.5 units from the 7th to the 30th day. FA can interact with carboxyl functional groups and consume protons, thereby increasing the soil pH [46]. MFA was more effective at enhancing the soil pH than FA with the same dosage due to the incorporation of Ca(OH)₂. Furthermore, higher amounts of aluminosilicate were released since the glassy structure of FA was destroyed after modification, which resulted in the increase of soil available Si in MFA-treated soils (Figure S2). A significant positive relationship was found between soil pH and soil available Si ($p < 0.01$) (Figure S3), indicating that the Si compounds may have been hydrolyzed in the soil and decarboxylated and released alkaline substances to enhance the buffering capacity of the soil [47,48].

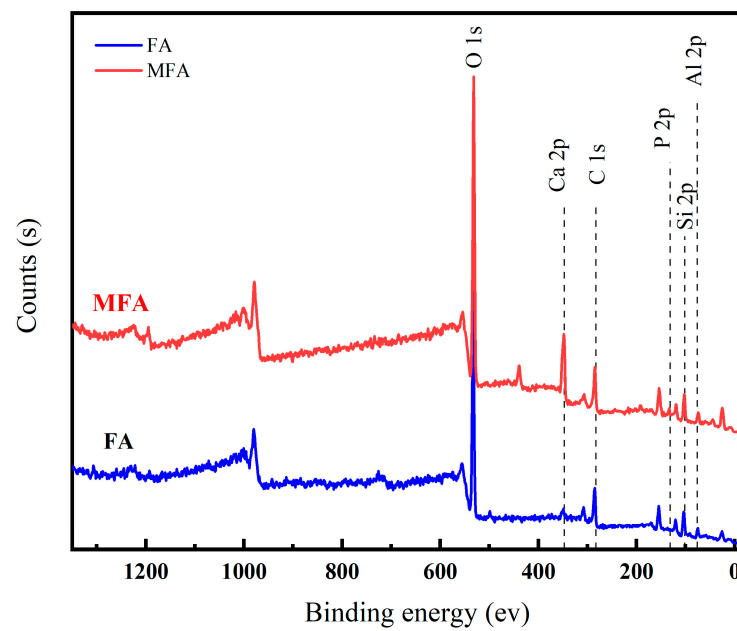


Figure 3. XPS full spectrum of FA and MFA. Note: FA: fly ash; MFA: modified fly ash.

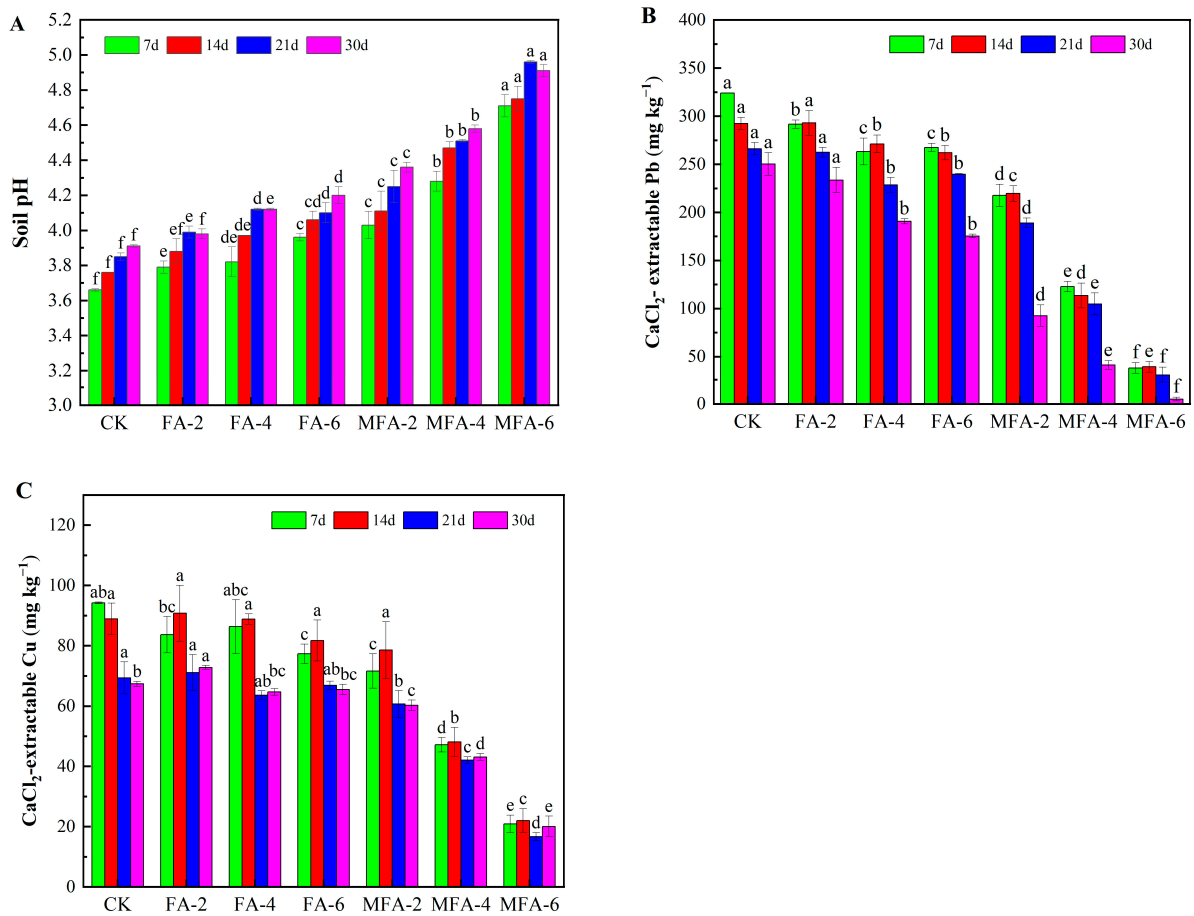


Figure 4. Changes in soil pH (A) and CaCl₂-extractable Pb (B) and Cu (C) in contaminated soil amended with FA or MFA. Note: CK, control soil; FA-2, 0.2% FA-treated soil; FA-4, 0.4% FA-treated soil; FA-6, 0.6% FA-treated soil; MFA-2, 0.2% MFA-treated soil; MFA-4, 0.4% MFA-treated soil; MFA-6, 0.6% MFA-treated soil. Different letters above the error bar indicate significant differences between the treatments ($p < 0.05$).

Moreover, the CaCl_2 -extractable Pb and Cu were significantly decreased with the increasing dosages of FA and MFA (Figure 4B,C). Compared to FA-treated soils, all MFA-treated soils significantly decreased CaCl_2 -extractable Pb and Cu by 25–97.1% and 13.5–75%, respectively. Arenas et al. [49] indicated that amorphous $\text{Ca}_3(\text{PO}_4)_2$ exhibits a notable adsorption effect for heavy metals. Although the phosphate minerals ($\text{Ca}_3(\text{PO}_4)_2$) were not identified in MFA by XRD, the immobilization efficiencies of Pb and Cu by MFA were higher than that of FA and the other alkline modification FA reported by previous studies [15,50,51]. For example, Hu et al. [50] used a alkali-modified FA with 4% dosage only decreased the soil available Pb and Cu by 62.7% and 48.1%, respectively. Furthermore, CaCl_2 -extractable Pb and Cu in all soils decreased with time, which may have been due to the continuous enhancement of soil pH (Figure 4A).

The Pb in the control soil was mainly presented in EXC and RES speciation, accounting for 59.7% and 23.6% of the total Pb, respectively (Table 1). FA and MFA significantly decreased the EXC-Pb compared to the control soil, and MFA significantly reduced EXC-Pb by 12.5–32% compared to FA. Meanwhile, 0.2–0.6% FA did not significantly change Pb in CA, OM, and RES speciation, but 0.4–0.6% MFA treatments significantly increased the Pb in CA, Fe-Mn, OM, and RES speciation by 9.31–27.1%, 52.5–98.7%, 69–97.9%, and 23.8–45.9%, respectively, compared to the control soil. Unlike Pb, Cu was mainly concentrated in RES (225 mg kg^{-1} , 34.8%) and Fe-Mn (212 mg kg^{-1} , 32.9%) speciation in the control soil, followed by EXC (119 mg kg^{-1} , 18.4%), CA (45.7 mg kg^{-1} , 7.1%), and OM (43.9 mg kg^{-1} , 6.8%) speciation. In addition, no FA treatments influenced EXC-Cu, but MFA significantly decreased EXC-Cu by 11.4–35.2% compared to FA. Compared to FA, 0.4–0.6% MFA treatments significantly increased Cu in CA and Fe-Mn speciation by 19.2–31.8% and 19.7–26%, respectively, but did not change Cu in OM or RES speciation.

Table 1. Chemical speciation of Pb and Cu in contaminated soil amended with FA and MFA.

Treatment		EXC	CA	Fe-Mn	OM	RES
Pb	CK	807 ± 4.98 ab	116 ± 0.04 cd	95.2 ± 3.14 d	15.1 ± 0.99 c	318 ± 0.71 d
	FA-2	797 ± 5.26 bc	109 ± 0.26 ef	75.4 ± 3.15 f	10.3 ± 0.70 d	324 ± 1.69 d
	FA-4	792 ± 11.92 c	115 ± 5.10 cde	78.1 ± 0.49 f	13.2 ± 0.70 c	323 ± 2.89 d
	FA-6	749 ± 7.60 d	113 ± 0.04 de	76.0 ± 1.35 f	12.8 ± 0.45 c	385 ± 4.28 b
	MFA-2	697 ± 0.52 e	122 ± 3.39 bc	120 ± 4.64 c	13.9 ± 0.54 c	374 ± 3.89 c
	MFA-4	631 ± 0.35 f	127 ± 2.79 b	145 ± 1.65 b	25.6 ± 2.14 b	394 ± 4.94 b
	MFA-6	510 ± 6.31 g	148 ± 3.85 a	189 ± 0.79 a	29.9 ± 1.14 a	464 ± 3.21 a
Cu	CK	119 ± 1.03 ab	45.7 ± 0.07 c	212 ± 0.94 b	43.9 ± 3.09 a	225 ± 4.40 cd
	FA-2	123 ± 2.12 a	43.1 ± 0.34 cd	190 ± 0.78 cd	36.5 ± 2.72 ab	228 ± 0.80 bcd
	FA-4	115 ± 4.78 b	44.6 ± 1.78 cd	190 ± 0.69 cd	40.0 ± 5.55 ab	234 ± 15.49 abcd
	FA-6	113 ± 1.87 bc	43.6 ± 0.47 cd	185 ± 3.20 d	41.4 ± 1.28 ab	248 ± 10.98 a
	MFA-2	108 ± 6.92 c	44.9 ± 0.71 cd	206 ± 3.55 b	35.6 ± 2.26 ab	244 ± 6.59 ab
	MFA-4	102 ± 1.65 d	53.2 ± 1.97 b	228 ± 7.48 a	33.5 ± 4.65 b	236 ± 10.06 abcd
	MFA-6	73.4 ± 1.73 e	57.4 ± 2.20 a	233 ± 7.39 a	43.4 ± 4.24 a	240 ± 2.35 abc

Note: CK, control soil; FA-2, 0.2% FA-treated soil; FA-4, 0.4% FA-treated soil; FA-6, 0.6% FA-treated soil; MFA-2, 0.2% MFA-treated soil; MFA-4, 0.4% MFA-treated soil; MFA-6, 0.6% MFA-treated soil. EXC, exchangeable; CA, bound to carbonate; Fe-Mn, iron and manganese oxide; OM, organic matter; RES, residual. Mean ($n = 3$) and standard error followed by different letters indicate significant differences ($p < 0.05$).

The above results indicate that MFA was more effective at decreasing the availability of Pb and Cu in soils than that of FA, which may be due to the following reasons. First, higher specific surface area in MFA can provide more adsorption sites than in FA [52]. Second, MFA was more effective at increasing soil pH, which can facilitate the passivation of heavy metals [15]. The significant negative correlation between soil pH and CaCl_2 -extractable and exchangeable Pb and Cu further verified the key role of soil pH ($p < 0.001$) (Figure S3). Third, amorphous Si/Al was formed, accompanied by the destruction of the glass-phase structure after modification of FA, which can enhance the adsorption capacities for Pb and Cu [53]. Previous studies have reported that amorphous Si can reduce the availability of heavy metals by transforming the metal speciation in soil solution into silicate complexes [54,55]. Fourth, phosphate could easily complex with heavy metals [56]; in particular, $\text{Ca}_3(\text{PO}_4)_2$

and CaCO_3 were newly formed in MFA, resulting in the formation of phosphate and carbonate precipitates of Pb and Cu [57]. Fifth, the stronger -OH and O-C-O functional groups in MFA would promote the formation of hydroxide and carbonate precipitate with Pb and Cu [58].

3.3. Ryegrass Growth and Heavy Metal Accumulation

Compared with the control, the application of both FA and MFA with 0.2–0.4% did not influence the dry biomass of the shoots of ryegrass, and only FA-6 and MFA-6 significantly increased the dry biomass of the roots of ryegrass by 25% and 30%, respectively ($p < 0.05$). Compared with the control soil, only FA-6 and MFA-6 significantly decreased the concentrations of Pb in the shoots of ryegrass by 22.7% and 35.9%, respectively ($p < 0.05$). All FA and MFA significantly decreased the concentrations of Pb in the roots of ryegrass by 22.7–26.9% and 30.1–31.3%, except for FA-2 and MFA-2, respectively ($p < 0.05$). MFA-4 and MFA-6 slightly decreased the concentrations of Pb in the shoots and roots of ryegrass by 9.97–17.1% and 6.1–9.55% compared to FA-4 and FA-6, respectively (Figure 5B). Moreover, no FA and MFA applications changed Cu uptake by the shoots of ryegrass compared to the control soil except for MFA-6. Similarly, only FA-6 significantly decreased the Cu in the roots of ryegrass by 32.6%, and MFA decreased the Cu in the roots of ryegrass by 30.6–53.6% compared to that of the control soil (Figure 5C). The results indicate that MFA slightly increased the biomass of ryegrass and decreased the uptake of Pb and Cu compared to those of FA. This may be due to the shorter time of the indoor incubation experiment and the application rates of MFA being significantly less than the rates reported by previous studies [48,50,59].

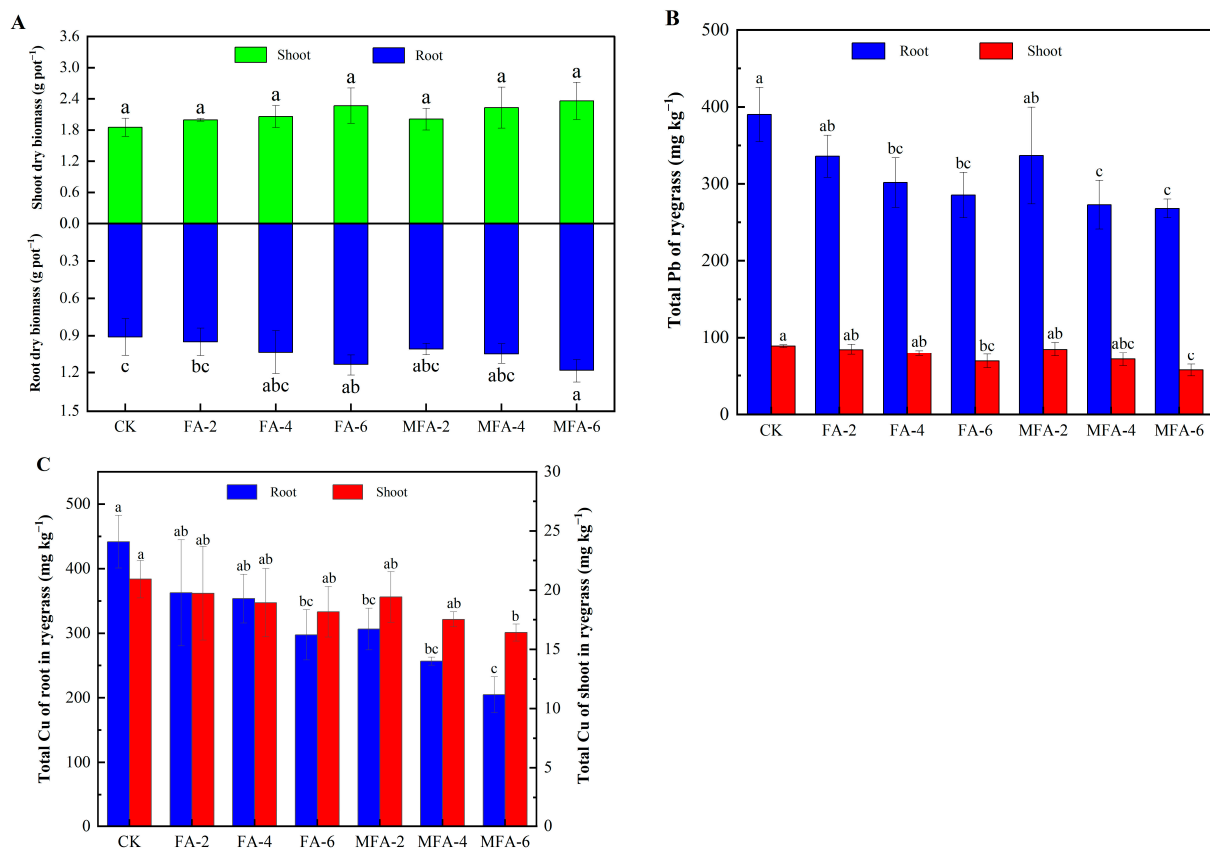


Figure 5. Effects of amendments application on the dry biomass of shoots and roots in ryegrass (A) and shoot and root Pb (B) and Cu (C) in ryegrass. Note: CK, control soil; FA-2, 0.2% FA-treated soil; FA-4, 0.4% FA-treated soil; FA-6, 0.6% FA-treated soil; MFA-2, 0.2% MFA-treated soil; MFA-4, 0.4% MFA-treated soil; MFA-6, 0.6% MFA-treated soil. Different letters above the error bar indicate significant differences between the treatments ($p < 0.05$).

As shown in Figure S4, the biomass of the shoots and roots of ryegrass were both significantly positively correlated with soil pH and available Si ($p < 0.05$). There was a significant negative correlation between soil pH and the uptake of Pb and Cu, except for the Pb in the roots of ryegrass ($p < 0.05$), which suggests that FA and MFA could significantly inhibit the Pb and Cu uptake in shoots of ryegrass by increasing soil pH [60,61]. Cu uptake by shoots and roots was positively correlated with soil available and exchangeable Pb and Cu ($p < 0.05$). Nevertheless, no significant relationships were observed between Pb uptake in ryegrass and soil available Pb ($p > 0.05$). Additionally, there were negative relationships between Pb and Cu uptake of ryegrass and soil available Si ($p < 0.05$). In general, the increase in available Si was facilitated by the decrease in available Pb and Cu in soil. This may be due to the co-precipitation of Si with metals and the increase in soil pH, which could decrease metal transport from root to shoot [55,62]. Nevertheless, the definite impact mechanisms of Si on the availability of heavy metals need to be further studied.

4. Conclusions

Compared with FA, MFA had more irregular agglomerates, which enhanced the specific surface area by 1.94 times. The modification process destroyed the glass-phase structure and destroyed the Si-O and Al-O active functional groups compared to the original FA. In the incubation experiment, MFA significantly increased soil pH by 0.23–0.86 units and was more effective at passivating Pb and Cu than FA by transforming the metals from active speciation to stable speciation. Moreover, SEM, BET, XRD, FTIR, and XPS showed that MFA could enhance the passivation of heavy metals by increasing specific surface area, functional groups, and the activation of Si. Besides, the increase in soil pH and the metal–phosphate precipitate were beneficial for metal passivation. Moreover, MFA slightly increased the dry biomass of shoots and roots and inhibited the accumulation of Pb and Cu in ryegrass compared to FA. Overall, MFA can be considered a potential passivation material for Pb- and Cu-contaminated soil, which has great significance for the utilization of FA.

Supplementary Materials: The following supporting information can be downloaded at: <https://www.mdpi.com/article/10.3390/agronomy13092194/s1>, Text S1: Characterization analysis; Text S2: Soil lead (Pb) and copper (Cu) sequential extraction procedure; Figure S1: Si2p and Al2p spectrum of FA (A) and MFA (B). Note: FA: fly ash; MFA: modified fly ash; Figure S2: Changes in available silicon (Si) in contaminated soil amended with FA or MFA. Note: CK, the control soil; FA-2, 0.2% FA treated soil; FA-4, 0.4% FA treated soil; FA-6, 0.6% FA treated soil; MFA-2, 0.2% MFA treated soil; MFA-4, 0.4% MFA treated soil; MFA-6, 0.6% MFA treated soil. Different letters above the error bar indicate significant differences between the treatments ($p < 0.05$); Figure S3: Correlations coefficients among soil pH, available Pb (A) and Cu (B), available Si, and Pb and Cu speciation. available Pb and Cu: CaCl₂-extractable-Pb and Cu, EXC, exchangeable; CA, bound to carbonates; Fe-Mn, bound to iron and manganese oxide oxides; OM, bound to organic matter; RES, residual. Note: ***: Significant correlation at the 0.001 level ($p < 0.001$). **: Significant correlation at the 0.01 level ($p < 0.01$). *: Significant correlation at the 0.05 level ($p < 0.05$); Figure S4: Correlation coefficients among soil pH, soil CaCl₂-extractable and exchangeable Pb and Cu, available Si, dry biomass in shoot and root ryegrass, accumulation of Pb and Cu in shoot and root ryegrass. C-Pb, CaCl₂-extractable-Pb; C-Cu, CaCl₂-extractable-Cu; EXC-Pb, exchangeable Pb; EXC-Cu, exchangeable Cu; A-Si, available Si; S-biomass, shoot dry biomass of ryegrass; R-biomass, root dry biomass of ryegrass; S-Pb, shoot Pb in ryegrass; R-Pb, root Pb in ryegrass; S-Cu, shoot Cu in ryegrass; R-Cu, root Pb in ryegrass. Note: ***: Significant correlation at the 0.001 level ($p < 0.001$). **: Significant correlation at the 0.01 level ($p < 0.01$). *: Significant correlation at the 0.05 level ($p < 0.05$).

Author Contributions: Conceptualization, writing—original draft, H.C., S.H., J.Z., S.Z. and X.S.; data curation, supervision, X.S., S.H. and H.C.; formal analysis, supervision, S.H. and H.C.; investigation, resources, H.C. and J.Z.; validation, visualization, S.Z., H.C. and X.S.; software, investigation, H.C., S.H., S.L. and J.Z. All authors have read and agreed to the published version of the manuscript.

Funding: This research was supported by the Anhui Province Natural Science Foundation (2208085MD87), the Natural Science Foundation of Universities of Anhui Province (KJ2020ZD35), the Academician Workstation in Anhui Province, Anhui University of Science and Technology (2022-AWAP-04), and the Key Scientific Research and Development Projects of Jiangxi Province (20194ABC28010).

Institutional Review Board Statement: Not applicable.

Informed Consent Statement: Not applicable.

Data Availability Statement: Not applicable.

Acknowledgments: Anonymous reviewers are acknowledged for their constructive comments and helpful suggestions.

Conflicts of Interest: The authors declare no conflict of interest.

References

1. Yao, Z.T.; Ji, X.S.; Sarker, P.K.; Tang, J.H.; Ge, L.Q.; Xia, M.S.; Xi, Y.Q. A comprehensive review on the applications of coal fly ash. *Earth-Sci. Rev.* **2015**, *141*, 105–121. [\[CrossRef\]](#)
2. Teng, X.; Liu, F.; Chiu, Y. The impact of coal and non-coal consumption on China's energy performance improvement. *Nat. Resour. Forum* **2020**, *44*, 334–352. [\[CrossRef\]](#)
3. Guo, X.; Wang, X.; Zheng, D. Effect of coal consumption on the upgrading of industrial structure. *Geofluids* **2022**, *2022*, 4313175. [\[CrossRef\]](#)
4. Blissett, R.S.; Rowson, N.A. A review of the multi-component utilisation of coal fly ash. *Fuel* **2012**, *97*, 1–23. [\[CrossRef\]](#)
5. Yan, F.; Jiang, J.; Li, K.; Liu, N.; Chen, X.; Gao, Y.; Tian, S. Green synthesis of nanosilica from coal fly ash and its stabilizing effect on CaO sorbents for CO₂ capture. *Environ. Sci. Technol.* **2017**, *51*, 7606–7615. [\[CrossRef\]](#)
6. Liu, F.; Ma, S.; Ren, K.; Wang, X. Mineralogical phase separation and leaching characteristics of typical toxic elements in Chinese lignite fly ash. *Sci. Total Environ.* **2020**, *708*, 135095. [\[CrossRef\]](#)
7. Dindi, A.; Quang, D.V.; Vega, L.F.; Nashef, E.; Abu-Zahra, M.R.M. Applications of fly ash for CO₂ capture, utilization, and storage. *J. CO₂ Util.* **2019**, *29*, 82–102. [\[CrossRef\]](#)
8. Izquierdo, M.; Querol, X. Leaching behaviour of elements from coal combustion fly ash: An overview. *Int. J. Coal Geol.* **2012**, *94*, 54–66. [\[CrossRef\]](#)
9. Han, D.; Xu, L.; Wu, Q.; Wang, S.; Duan, L.; Wen, M.; Li, Z.; Tang, Y.; Li, G.; Liu, K. Potential environmental risk of trace elements in fly ash and gypsum from ultra-low emission coal-fired power plants in China. *Sci. Total Environ.* **2021**, *798*, 149116. [\[CrossRef\]](#)
10. Luo, Y.; Wu, Y.; Ma, S.; Zheng, S.; Zhang, Y.; Chu, P.K. Utilization of coal fly ash in China: A mini-review on challenges and future directions. *Environ. Sci. Pollut. Res.* **2021**, *28*, 18727–18740. [\[CrossRef\]](#)
11. Mushtaq, F.; Zahid, M.; Bhatti, I.A.; Nasir, S.; Hussain, T. Possible applications of coal fly ash in wastewater treatment. *J. Environ. Manag.* **2019**, *240*, 27–46. [\[CrossRef\]](#) [\[PubMed\]](#)
12. Alinnor, I.J. Adsorption of heavy metal ions from aqueous solution by fly ash. *Fuel* **2007**, *86*, 853–857. [\[CrossRef\]](#)
13. Buema, G.; Harja, M.; Lupu, N.; Chiriac, H.; Forminte, L.; Ciobanu, G.; Bucur, D.; Bucur, R.D. Adsorption performance of modified fly ash for copper ion removal from aqueous solution. *Water* **2021**, *13*, 207. [\[CrossRef\]](#)
14. Cui, H.; Wu, Q.; Zhang, X.; Su, B.; Yi, Q.; Zhang, S.; Zhou, J. Stabilization of copper and cadmium in contaminated soil by fly ash. *Soil* **2016**, *48*, 971–977. (In Chinese)
15. Xu, D.; Ji, P.; Wang, L.; Zhao, X.; Hu, X.; Huang, X.; Zhao, H.; Liu, F. Effect of modified fly ash on environmental safety of two soils contaminated with cadmium and lead. *Ecotoxicol. Environ. Saf.* **2021**, *215*, 112175. [\[CrossRef\]](#)
16. Deng, X.; Qi, L.; Zhang, Y. Experimental study on adsorption of hexavalent chromium with microwave-assisted alkali modified fly ash. *Water Air Soil Pollut.* **2018**, *229*, 18. [\[CrossRef\]](#)
17. Zhao, Y.; Luan, H.; Yang, B.; Li, Z.; Song, M.; Li, B.; Tang, X. Adsorption of Pb, Cu and Cd from water on coal fly ash-red mud modified composite material: Characterization and mechanism. *Water* **2023**, *15*, 767. [\[CrossRef\]](#)
18. Pan, Y.; Liu, G.; Chai, B.; Lei, X.; He, L.; Cheng, S.; Wang, Y.; Chen, W.; Li, S.; Chen, L.; et al. Control of endogenous phosphorus release at the sediment-water interface by lanthanum-modified fly ash. *Coatings* **2022**, *12*, 719. [\[CrossRef\]](#)
19. Huang, X.; Zhao, H.; Zhang, G.; Li, J.; Yang, Y.; Ji, P. Potential of removing Cd(II) and Pb(II) from contaminated water using a newly modified fly ash. *Chemosphere* **2020**, *242*, 125148. [\[CrossRef\]](#)
20. Cui, H.; Zhang, X.; Wu, Q.; Zhang, S.; Xu, L.; Zhou, J.; Zheng, X.; Zhou, J. Hematite enhances the immobilization of copper, cadmium and phosphorus in soil amended with hydroxyapatite under flooded conditions. *Sci. Total Environ.* **2020**, *708*, 134590. [\[CrossRef\]](#)
21. Barsbay, M.; Kavakh, P.A.; Tilki, S.; Kavakh, C.; Guven, O. Porous cellulosic adsorbent for the removal of Cd(II), Pb(II) and Cu(II) ions from aqueous media. *Radiat. Phys. Chem.* **2018**, *142*, 70–76. [\[CrossRef\]](#)
22. Hoang, T.T.T.L.; Unob, F.; Suvokhiaw, S.; Sukpirom, N. One-pot synthesis of amorphous calcium phosphate/Fe₃O₄ composites and the application in the removal of cadmium. *J. Environ. Chem. Eng.* **2020**, *8*, 103653. [\[CrossRef\]](#)

23. Cao, X.; Liang, Y.; Zhao, L.; Le, H. Mobility of Pb, Cu, and Zn in the phosphorus-amended contaminated soils under simulated landfill and rainfall conditions. *Environ. Sci. Pollut. Res.* **2013**, *20*, 5913–5921. [[CrossRef](#)]
24. Cui, H.; Zhang, S.; Li, R.; Yi, Q.; Zheng, X.; Hu, Y.; Zhou, J. Leaching of Cu, Cd, Pb, and phosphorus and their availability in the phosphate-amended contaminated soils under simulated acid rain. *Environ. Sci. Pollut. Res.* **2017**, *24*, 21128–21137. [[CrossRef](#)]
25. Cui, H.; Fan, Y.; Xu, L.; Zhou, J.; Zhou, D.; Mao, J.; Fang, G.; Cang, L.; Zhu, Z. Sustainability of in situ remediation of Cu- and Cd-contaminated soils with one-time application of amendments in Guixi, China. *J. Soils Sediments* **2016**, *16*, 1498–1508. [[CrossRef](#)]
26. Cui, H.; Li, D.; Liu, X.; Fan, Y.; Zhang, X.; Zhang, S.; Zhou, J.; Fang, G.; Zhou, J. Dry-wet and freeze-thaw aging activate endogenous copper and cadmium in biochar. *J. Clean Prod.* **2021**, *288*, 125605. [[CrossRef](#)]
27. Walkley, A.; Black, I.A. An examination of the Degtjareff method for determining soil organic matter, and a proposed modification of the chromic acid titration method. *Soil Sci.* **1934**, *37*, 29–38. [[CrossRef](#)]
28. Pansu, M.; Gautheyrou, J. *Handbook of Soil Analysis: Mineralogical, Organic and Inorganic Methods*; Springer: Berlin, Germany; New York, NY, USA, 2006.
29. Li, Z.; Unzué-Belmonte, D.; Cornelis, J.T.; Linden, C.V.; Struyf, E.; Ronsse, F.; Delvaux, B. Effects of phytolith rice-straw biochar, soil buffering capacity and pH on silicon bioavailability. *Plant Soil.* **2019**, *438*, 187–203. [[CrossRef](#)]
30. Cui, H.; Fan, Y.; Fang, G.; Zhang, H.; Su, B.; Zhou, J. Leachability, availability and bioaccessibility of Cu and Cd in a contaminated soil treated with apatite, lime and charcoal: A five-year field experiment. *Ecotoxicol. Environ. Saf.* **2016**, *134*, 148–155. [[CrossRef](#)]
31. Cui, H.; Dong, T.; Hu, L.; Xia, R.; Zhou, J.; Zhou, J. Adsorption and immobilization of soil lead by two phosphate-based biochars and phosphorus release risk assessment. *Sci. Total Environ.* **2022**, *824*, 153957. [[CrossRef](#)]
32. Tessier, A.; Campbell, P.G.C.; Bisson, M. Sequential extraction procedure for the speciation of particulate trace metals. *Anal. Chem.* **1979**, *51*, 844–851. [[CrossRef](#)]
33. Cui, H.; Cheng, J.; Shen, L.; Zheng, X.; Zhou, J.; Zhou, J. Activation of endogenous cadmium from biochar under simulated acid rain enhances the accumulation risk of lettuce (*Lactuca Sativa* L.). *Ecotoxicol. Environ. Saf.* **2023**, *255*, 114820. [[CrossRef](#)] [[PubMed](#)]
34. Yang, B.; Ma, S.; Cui, R.; Sun, S.; Wang, J.; Li, S. Simultaneous removal of NO_x and SO₂ with H₂O₂ catalyzed by alkali/magnetism-modified fly ash: High efficiency, low cost and catalytic mechanism. *Chem. Eng. J.* **2019**, *359*, 233–243. [[CrossRef](#)]
35. Phair, J.W.; van Deventer, J.S.J. Characterization of fly-ash-based geopolymeric binders activated with sodium aluminate. *Ind. Eng. Chem. Res.* **2002**, *41*, 4242–4251. [[CrossRef](#)]
36. Yang, Y.; Wang, L.; Zhao, H.; Yan, F.; Li, S.; Guo, B.; Lue, C.; Huang, X.; Ji, P. Utilization of KOH-modified fly ash for elimination from aqueous solutions of potentially toxic metal ions. *Environ. Res.* **2023**, *223*, 115396. [[CrossRef](#)] [[PubMed](#)]
37. Ameh, A.E.; Musyoka, N.M.; Fatoba, O.O.; Syrtsova, D.A.; Teplyakov, V.V.; Petrik, L.F. Synthesis of zeolite NaA membrane from fused fly ash extract. *J. Environ. Sci. Health Part A-Toxic Hazard. Subst. Environ. Eng.* **2016**, *51*, 348–356. [[CrossRef](#)]
38. Zhao, H.; Huang, X.; Zhang, G.; Li, J.; He, Z.; Ji, P.; Zhao, J. Possibility of removing cadmium pollution from the environment using a newly synthesized material coal fly ash. *Environ. Sci. Pollut. Res.* **2020**, *27*, 4997–5008. [[CrossRef](#)]
39. Yeheyis, M.B.; Shang, J.Q.; Yanful, E.K. Characterization and environmental evaluation of atikokan coal fly ash for environmental applications. *J. Environ. Eng. Sci.* **2008**, *7*, 481–498. [[CrossRef](#)]
40. Barani, K.; Koleini, S.M.J.; Rezaei, B. Magnetic properties of an iron ore sample after microwave heating. *Sep. Purif. Technol.* **2011**, *76*, 331–336. [[CrossRef](#)]
41. Chen, X.; Zhang, G.; Li, J.; Ji, P. Possibility of removing Pb and Cd from polluted water by modified fly ash. *Adsorpt. Sci. Technol.* **2021**, *2021*, 1336638. [[CrossRef](#)]
42. Cretescu, I.; Harja, M.; Teodosiu, C.; Isopescu, D.N.; Chok, M.F.; Sluser, B.M.; Salleh, M.A.M. Synthesis and characterisation of a binder cement replacement based on alkali activation of fly ash waste. *Process Saf. Environ. Prot.* **2018**, *119*, 23–35. [[CrossRef](#)]
43. Wang, K.; Peng, N.; Sun, J.; Lu, G.; Chen, M.; Deng, F.; Dou, R.; Nie, L.; Zhong, Y. Synthesis of silica-composited biochars from alkali-fused fly ash and agricultural wastes for enhanced adsorption of methylene blue. *Sci. Total Environ.* **2020**, *729*, 139055. [[CrossRef](#)] [[PubMed](#)]
44. Omran, M.; Fabritius, T.; Elmahdy, A.M.; Abdel-Khalek, N.A.; El-Aref, M.; Elmanawi, A. XPS and FTIR spectroscopic study on microwave treated high phosphorus iron ore. *Appl. Surf. Sci.* **2015**, *345*, 127–140. [[CrossRef](#)]
45. Li, Z.; Wang, L.; Meng, J.; Liu, X.; Xu, J.; Wang, F.; Brookes, P. Zeolite-supported nanoscale zero-valent iron: New findings on simultaneous adsorption of Cd(II), Pb(II), and As(III) in aqueous solution and soil. *J. Hazard. Mater.* **2018**, *344*, 1–11. [[CrossRef](#)] [[PubMed](#)]
46. Hu, X.; Yuan, X.; Dong, L. Coal fly ash and straw immobilize Cu, Cd and Zn from mining wasteland. *Environ. Chem. Lett.* **2014**, *12*, 289–295. [[CrossRef](#)]
47. Pizarro, J.; Castillo, X.; Jara, S.; Ortiz, C.; Navarro, P.; Cid, H.; Rioseco, H.; Barros, D.; Belzile, N. Adsorption of Cu²⁺ on coal fly ash modified with functionalized mesoporous silica. *Fuel* **2015**, *156*, 96–102. [[CrossRef](#)]
48. Liu, F.; Huang, X.; Zhao, H.; Hu, X.; Wang, L.; Zhao, X.; Gao, P.; Ji, P. Stabilization of Cd and Pb in the contaminated soils by applying modified fly ash. *Soil Ecol. Lett.* **2021**, *3*, 242–252. [[CrossRef](#)]
49. Arenas-Lago, D.; Rodriguez-Seijo, A.; Lago-Vila, M.; Andrade Couce, L.; Vega, F.A. Using Ca₃(PO₄)₂ nanoparticles to reduce metal mobility in shooting range soils. *Sci. Total Environ.* **2016**, *571*, 1136–1146. [[CrossRef](#)]
50. Hu, X.; Huang, X.; Zhao, H.; Liu, F.; Wang, L.; Zhao, X.; Gao, P.; Li, X.; Ji, P. Possibility of using modified fly ash and organic fertilizers for remediation of heavy-metal-contaminated soils. *J. Clean. Prod.* **2021**, *284*, 124713. [[CrossRef](#)]

51. Yan, F.; Zhao, H.; Liu, F.; Wang, L.; Huang, X.; Zhao, X.; Yang, Y.; Li, J.; Zhang, G.; Ju, X.; et al. Remediation of cadmium and lead in contaminated soils by a newly modified fly ash material: The possibility and safety. *Environ. Technol. Innov.* **2022**, *28*, 102894. [[CrossRef](#)]
52. Wang, L.; Huang, X.; Zhang, J.; Wu, F.; Liu, F.; Zhao, H.; Hu, X.; Zhao, X.; Li, J.; Ju, X.; et al. Stabilization of lead in waste water and farmland soil using modified coal fly ash. *J. Clean. Prod.* **2021**, *314*, 127957. [[CrossRef](#)]
53. Khalid, H.R.; Lee, N.K.; Choudhry, I.; Wang, Z.; Lee, H.K. Evolution of zeolite crystals in geopolymer-supported zeolites: Effects of composition of starting materials. *Mater. Lett.* **2019**, *239*, 33–36. [[CrossRef](#)]
54. Khan, I.; Awan, S.A.; Rizwan, M.; Ali, S.; Hassan, M.J.; Brestic, M.; Zhang, X.; Huang, L. Effects of silicon on heavy metal uptake at the soil-plant interphase: A review. *Ecotoxicol. Environ. Saf.* **2021**, *222*, 112510. [[CrossRef](#)]
55. Bhat, J.A.; Shivaraj, S.M.; Singh, P.; Navadagi, D.B.; Tripathi, D.K.; Dash, P.K.; Solanke, A.U.; Sonah, H.; Deshmukh, R. Role of silicon in mitigation of heavy metal stresses in crop plants. *Plants* **2019**, *8*, 71. [[CrossRef](#)] [[PubMed](#)]
56. Wan, B.; Yan, Y.; Tang, Y.; Bai, Y.; Liu, F.; Tan, W.; Huang, Q.; Feng, X. Effects of polyphosphates and orthophosphate on the dissolution and transformation of ZnO nanoparticles. *Chemosphere* **2017**, *176*, 255–265. [[CrossRef](#)] [[PubMed](#)]
57. Cao, X.; Ma, L.Q.; Chen, M.; Singh, S.P.; Harris, W.G. Impacts of phosphate amendments on lead biogeochemistry at a contaminated site. *Environ. Sci. Technol.* **2002**, *36*, 5296–5304. [[CrossRef](#)] [[PubMed](#)]
58. Gao, R.; Hu, H.; Fu, Q.; Li, Z.; Xing, Z.; Ali, U.; Zhu, J.; Liu, Y. Remediation of Pb, Cd, and Cu contaminated soil by co-pyrolysis biochar derived from rape straw and orthophosphate: Speciation transformation, risk evaluation and mechanism inquiry. *Sci. Total Environ.* **2020**, *730*, 139119. [[CrossRef](#)]
59. Zhao, H.; Huang, X.; Liu, F.; Hu, X.; Zhao, X.; Wang, L.; Gao, P.; Li, X.; Ji, P. Potential of using a new aluminosilicate amendment for the remediation of paddy soil co-contaminated with Cd and Pb. *Environ. Pollut.* **2021**, *269*, 116198. [[CrossRef](#)]
60. Contin, M.; Miho, L.; Pellegrini, E.; Gjoka, F.; Shkurta, E. Effects of natural zeolites on ryegrass growth and bioavailability of Cd, Ni, Pb, and Zn in an Albanian contaminated soil. *J. Soils Sediments* **2019**, *19*, 4052–4062. [[CrossRef](#)]
61. Jakubus, M.; Graczyk, M. The effect of compost and fly ash treatment of contaminated soil on the immobilisation and bioavailability of lead. *Agronomy* **2021**, *11*, 1188. [[CrossRef](#)]
62. Gu, H.; Qiu, H.; Tian, T.; Zhan, S.; Deng, T.; Chaney, R.L.; Wang, S.; Tang, Y.; Morel, J.; Qiu, R. Mitigation effects of silicon rich amendments on heavy metal accumulation in rice (*Oryza sativa* L.) planted on multi-metal contaminated acidic soil. *Chemosphere* **2011**, *83*, 1234–1240. [[CrossRef](#)] [[PubMed](#)]

Disclaimer/Publisher’s Note: The statements, opinions and data contained in all publications are solely those of the individual author(s) and contributor(s) and not of MDPI and/or the editor(s). MDPI and/or the editor(s) disclaim responsibility for any injury to people or property resulting from any ideas, methods, instructions or products referred to in the content.